From CT Scan to Plantar Pressure Map Distribution of a 3D Anatomic Human Foot

P. Franciosa, S. Gerbino*
University of Molise, School of Engineering
*Corresponding author: Via Duca degli Abruzzi - 86039 Termoli (CB) – Italy
salvatore.gerbino@unimol.it

Abstract: Understanding the stress-strain behavior of human foot tissues and pressure map distributions at the plantar interface is of interest into biomechanical investigations. In particular, monitoring plantar pressure maps is crucial to establishing the perceived human comfort of shoe insoles.
In this contest, a 3D anatomical detailed FE human foot model was created, starting from CT (Computer Tomography) scans of a 29 years old male. Anatomical domains related to bones and soft tissues were generated, using segmentation techniques, and then processed into a CAD environment to model 3D domains by using loft/sweep and boolean operations. Finally, FE model was generated into Comsol Multiphysics® 3.5a, by assigning contact pairs and defining non-linear material laws. Particular attention was posed on fine tuning the calculation strongly dependent on the convergence parameters influenced by the contacts and hyper-elastic material properties.

Keywords: CT scan, CAD foot model, hyper-elastic material, contact analysis, plantar pressure map.

1. Introduction

It was reported that the perceived comfort related to the human foot can be associated to the contact pressure generated at the plantar - insole interface [1]. High values of pressure can generate pain or pathologies due to the obstruction of blood circulation in areas with peak values of pressure. Experimental studies have pointed out a relationship between perceived comfort and plantar pressures [2], [3]. Over years, many researchers have addressed their attention on minimizing the plantar pressure, by varying insole footwear materials, thickness and anatomical shape [4], [5], [6].

Recently, in order to give a valuable support to experimental investigations, computational methods, based on FE modeling, have also been adopted. FE models of human foot have been developed under certain simplifications and assumptions (see [7] and [8]) such as: (i) simplified or partial foot shape, (ii) assumptions of non-linear hyper-elastic material law, (iii) ligaments and plantar fascia modeled as equivalent forces or elastic beams/bars, (iiii) no friction or thermal effect, at plantar foot interface, accounted.

Based on these assumptions, valuable 3D FE models were presented in the literature [9], [10]. In this contest, the geometrical complexity of foot structure was captured through reverse engineering methodologies, based on CT (Computer Tomography) or MR (Magnetic Resonance) scans. Starting from high resolution medical images, suitable FE models were generated by using segmentation procedures.

In the present paper, how to face out the 3D geometry reconstruction of the human foot into Comsol Multiphisics® 3.5a is investigated. Comsol Multiphisics® offers a direct link with two of the most powerful commercial tools able to generate 3D tetrahedral mesh models starting from stack-up images: ScanFE® (by Simpleware®) and Mimics® (by Materialise®) [11]. However, as reported and experimented yet in [12], so-imported mesh models cannot be edited in Comsol Multiphisics®. This program, when working on tessellated geometries, creates rational Bezier patches, defining boundary or domain equations. Manipulating or editing those boundaries/domains, which requires geometry decomposition analysis, is not allowed.

To avoid all these crucial issues, one should create B-rep CAD geometry starting from segmented surfaces, extracted from stack-up images. If, on one hand, this stage may be time consuming, on the other hand a suitable CAD geometry model is finally available and ready to be post-processed into any multiphysic simulation.

The above approach was adopted, for example, into [13], where, starting from MR scans, the foot geometry was created and then assembled

into SolidWorks® CAD system.

In the present paper, the development of the detailed 3D anatomic FE model of a human foot is described. The balanced standing condition was simulated: the foot was supposed to be touching an ideal-rigid ground. Hyper-elastic material law was assigned to soft tissues. Contact pressures were calculated by adopting a non-linear static simulation. How to speed-up the solution convergence by fine-tuning non-linear tolerance, penalty factor and scaling value, was also highlighted.

2. Methodology Overview

Figure 1 depicts the general work-flow adopted in the present research.

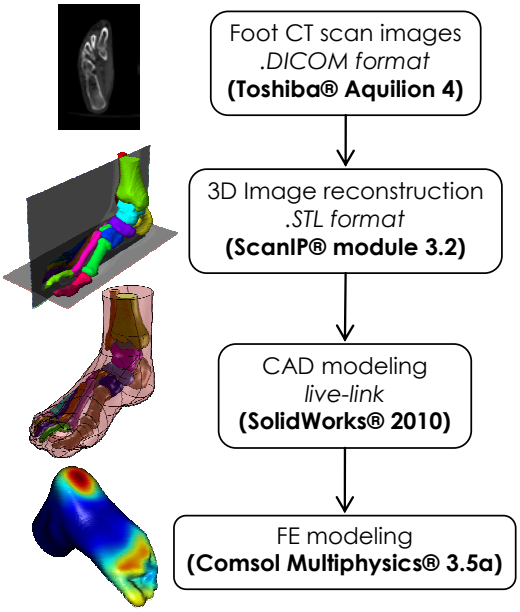

Figure 1. Work-flow methodology

A 29 years old male was submitted to a CT scan. Medical images of both feet were imported into ScanIP® module of Simplewere® software, where bones and soft tissues were extracted by adopting density-based segmentation procedures. At this stage boundary surfaces, into the tessellated format, were generated. Those surfaces were, then, exported into .STL format and imported into SolidWorks® CAD system. Here, solid domains were generated by adopting loft/sweep and boolean operations. From this CAD model, the FE model was created directly into Comsol Multiphisics® for the non-linear analysis, by using the live-link between both environments. Boundary conditions, contact and identity pairs were introduced. Domain equations were set to simulate the non-linear hyper-elastic behavior of the foot soft tissue.

3. Foot Modeling

A CT (Toshiba® Aquilion 4 equipment) scan was performed on a 29 years old male (65 Kg). 345 slices were captured with a slice distance of 1.0 mm (see Figure 2.a).

Scans were made for both feet in their neutral posture in which there is the least tension or pressure on tendons, muscles and bones.

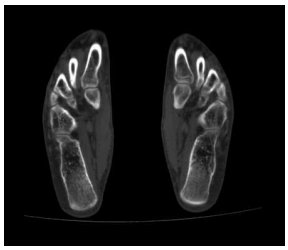

Figure 2.a. DICOM image

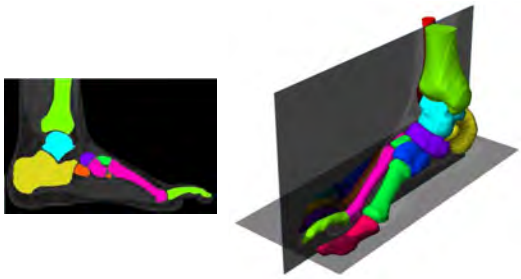

2D segmented regions 3D reconstructed domains

Figure 2.b. Segmented regions and 3D reconstruction

Medical images were, then, exported into standard .DICOM format (image resolution 512x512 pixels) and processed by using ScanIP® tools. Generally speaking, DICOM images are gray-based images. Different gray-levels correspond to different density materials (Figure 2.b). Looking at DICOM images the following regions can be distinguished: soft tissue, bone, ligaments, plantar fascia and cartilages. In the present paper, only bones and soft tissue were segmented. Ligaments and plantar fascia were added at FEM stage as equivalent

load conditions (see also Section 4); instead, cartilages were modeled separately at CAD stage. In order to reduce the reconstruction effort, slice pixels related to left foot were removed. Thus, in the following only the right foot will be analyzed.

Figures 3.a and 3.b show the assembled bone structure and the soft tissue domain as seen into ScanIP® environment, respectively. Bone structure was composed of 19 bones: tibia, fibula, talus, calcaneus, cuboid, navicular, 3 cuneiforms (bones of the metatarsus), 5 metatarsals (bones of the metatarsus) and 5 components of the phalanges (bones of the toes). Phalange bones (a proximal and a distal phalanx for the great toe; proximal, middle and distal phalanges for the second to fifth toes) were fused together since their relative motion do not affect plantar pressures.

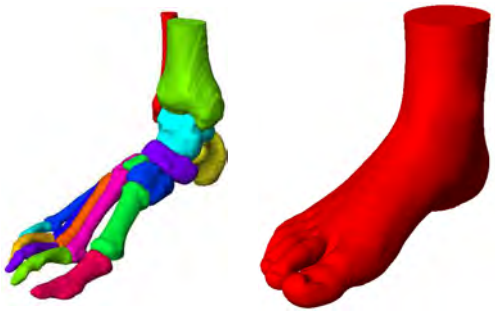

a. Bone structure **b**. Soft tissue

Figure 3. Tessellated surfaces generated into ScanIP® environment

One should note that the so-generated domains are geometrically described by the tessellated boundary surfaces.

These tessellated models were then imported into SolidWorks® CAD system by using the SCANto3D® add-in module to process and manage imported tessellated surfaces.

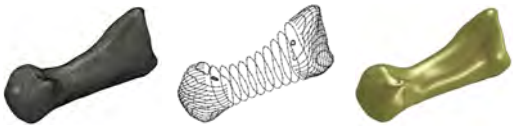

a b c

Figure 4. Generation of CAD model. a: tessellated geometry; b: cross-section curves; c: 3D CAD model

Starting from cross-sections (created as intersection curves between cut planes and the tessellated surfaces), lofting/sweeping/filling surfaces were generated as also described in [14].

Figure 4 shows the typical work-flow (first metatarsal bone used as example) adopted to generate solid domains, starting from cross-section curves.

CAD procedure is based on the following criteria:

- minimum number of surface patches; and,
- surface patches large as much as possible.

All this assures more flexibility in handling 3D mesh and boundary conditions at FEM stage.

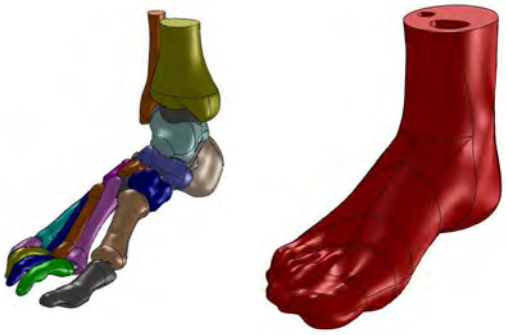

a. Bone structure **b**. Soft tissue

Figure 5. 3D CAD domains generated into SolidWorks®

Figure 5 depicts the so-reconstructed CAD geometry. Cartilages that were not extracted into the segmentation phase were then modeled into the CAD system in order to joint bones and fill the cartilaginous space (see Figure 5.a). Boolean operations were used to ensure congruence among the related interfacial surfaces. For instance, the whole bone structure was subtracted from the soft tissue. Finally, toes at soft tissue level were merged together (Figure 5.b).

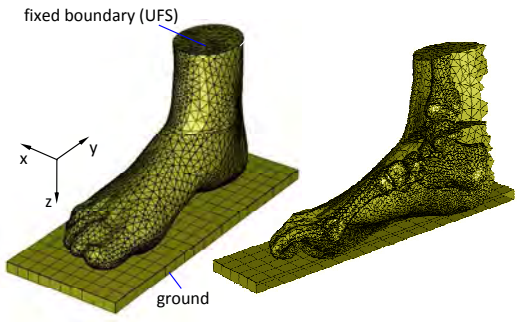

Figure 6. FE model as seen into Comsol Multiphisics®

4. FE Modeling

The foot CAD model was thus imported into Comsol Multiphisics® 3.5a, by using the live-link connection with SolidWorks®.

Here, domain equations, boundary conditions and solver settings were provided.

In the present paper the balanced standing condition was simulated. The foot was supposed to touch an ideal-rigid flat ground. For this purpose the "ground" domain was added to the FE model (see Figure 6).

4.1 Domain Equations

Materials were assumed linear and isotropic, while the soft tissue was modeled as a non-linear hyper-elastic material. As reported into [7], the material law, which best represents the compressibility and the highly non-linear behavior of soft tissue, is a polynomial law, as stated into relationship (1), where C_{ij} (N/m^2) and d_k (m^2/N) are the material constants. II_1, II_2 and J are the first, the second and the third modified strain invariants, respectively. W is the strain energy per unit of volume.

$$\begin{aligned} W(II_1, II_2, J) &= C_{10}\cdot(II_1-3)+C_{01}\cdot(II_2-3)+... \\ &...+C_{20}\cdot(II_1-3)^2+C_{11}\cdot(II_1-3)\cdot(II_2-3)+... \\ &...+C_{02}\cdot(II_2-3)^2+\frac{1}{D_1}\cdot(J-1)^2+\frac{1}{D_2}\cdot(J-1)^4 \end{aligned} \quad (1)$$

Material constants, reported in Table 1, were derived from *in vivo* tests in [7]. Equation (1) can be easily implemented into Comsol Multiphisics® as a domain equation.

Constant	Value
C_{10} (N/m^2)	85550.0
C_{01} (N/m^2)	-58400.0
C_{20} (N/m^2)	38920.0
C_{11} (N/m^2)	-23100.0
C_{02} (N/m^2)	8484.0
D_1 (m^2/N)	0.4370e-5
D_2(m^2/N)	0.6811e-6

Table 1. Material constants for human soft tissue [7]

Table 2 reports material constants for bone and cartilage domains ("E" is the Young's modulus, while "ν" is the Poisson's ratio).

Constant	Value
E_{bone} (MPa)	7300.0
$E_{cartilage}$ (MPa)	10.0
ν_{bone}	0.30
$\nu_{cartilage}$	0.40

Table 2. Material constants for bones and cartilages [7]

4.2 Boundary Conditions

During the balanced standing condition, a vertical force, corresponding to one half of the body weight (F_w=650/2 N), is transferred from the body to the foot and then to the ground.

The plantar fascia stabilizes the longitudinal arch of the foot and supports the longitudinal forces during the weight application phase [8]. As discussed in Section 3, plantar fascia was geometrically simplified and modeled at FEM stage by defining equivalent longitudinal forces.

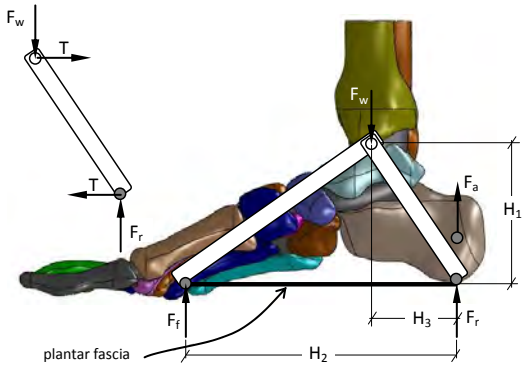

Figure 7. 2D model for the estimation of plantar fascia force
H_1=58.74 mm, H_2=140.49 mm, H_3=32.67 mm

A 2D equivalent model was adopted, as suggested also in [8], to estimate those forces. Looking at Figure 7, the longitudinal force T may be evaluated once F_r (force exerted at rear-foot) or F_f (force exerted at fore-foot) is known. From simple considerations about the 2D static equilibrium, one can write:

$$\begin{cases} F_r = \dfrac{F_w\cdot(H_2 - H_3)}{H_2} \\ T\cdot H_1 = F_r\cdot H_3 \end{cases} \rightarrow T = \frac{F_w\cdot(H_2-H_3)}{H_2}\cdot\frac{H_3}{H_1} \quad (2)$$
$$T = 0.4268\cdot F_w$$

Equation (2) says that about 42% of the applied weight, F_w, is supported by the plantar fascia.

Assuming that the force T is equally supported by all metatarsal bones, then, the net traction force to be applied to every metatarsal bone equals about 9% of the applied weight.

Furthermore, as suggested into [10] and [13], the Achilles' tendon force, F_a, may be assumed equal to about 75% of the applied weight.
Finally, to the upper surfaces (UFS into Figure 6) of soft tissue, tibia and fibula fixed constraints were applied.

Figure 8. Definition of identity pairs on the colored surfaces

Physical interaction among bones-soft tissue and bones-cartilages was modeled by defining identity pairs among interfacial surfaces. All this assures that the displacement fields at interfacial surfaces are identical each-other. Figure 8 depicts the so-defined identity pairs.

4.2 Contact Pair Modeling

Since plantar pressures are also of interest, contact pairs among plantar surfaces and ground-surface were defined (Figure 9). Moreover, no friction was accounted in the analysis.

Foot and ground were supposed to be not in contact initially: a small gap was left among contact surfaces. To face out this kind of problem, the initial contact pressure, the scaling factor and the penalty factor have to be set properly. These factors strongly influence the convergence process and its speed.

Since master and slave surfaces are initially not in contact, zero initial contact pressure was assumed. The scaling factor, s_f, related to the contact variable was chosen equal to $s_f=F_w/A_c$, where F_w and A_c are the applied weight and the estimated final contact area, respectively. Choosing the right A_c value is not a trivial task. Several experiments (with a "trial and error" approach) were conducted to carry out the optimal scaling factor, allowing to reach a valid solution problem into a reasonable time.

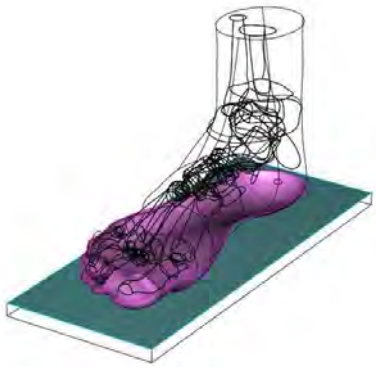

Figure 9. Definition of contact pairs between colored surfaces

The penalty factor, p_n, may aid the solver to get started and to speed the convergence up. Generally speaking, p_n depends on several factors, such as mesh size and material law parameters [15]. In the present paper, p_n was chosen equal to $p_n=s_c \cdot E_e/h_{mesh}$, where h_{mesh} is the mean mesh size, E_e is an equivalent elastic modulus and s_c is a correction factor. E_e modulus was set equal to $E_e=(C_{10}+C_{20})/2$, where C_{10} and C_{20} are the first and the third constant of the chosen hyper-elastic material (see relationship (1)), respectively. The s_c factor was assumed equal to 10.0. One should note that if, on one hand, a high penalty factor speeds the convergence process up, on the other hand the global stiffness matrix may be ill-conditioned. Thus, choosing the optimal penalty factor is a crucial task to be achieved when facing out contact problems.

Another feature to be considered, when managing and solving contact problems, is the constraint status of each domain. Authors have experimented that "lack of constraints" causes problems with the convergence process into Comsol Multiphysics®. Therefore, is it important that all domains are constrained in all directions, so that there is only one possible solution for each convergence iteration. For this reason, the ground domain was supposed to rigidly move only along the global Z direction (see Figure 6) starting from a distance of about 1 mm from the foot. In this way, all domains are properly con-

strained, and unwanted rigid motions are avoided.

5. FE Solution and Results

FE model was resolved by adopting a non-linear solver ("PARDISO out of core" was used as linear system solver).

To aid convergence process when calculating contact variables, a parametric solver was also adopted. As discussed above, the ground displacement along Z direction was parameterized to linearly change into the range [0, w_{max}]. The w_{max} value was chosen so that the reaction force calculated at UFS was greater or equal to the applied weight, F_w. So, w_{max}=8.0 mm was a good guess.

When facing out contact problems, also the tolerance (N_{tol}) for non-linear solver has to be properly set. As suggested into [16], the following condition should be satisfied:

$$N_{tol} \leq \frac{s_f \cdot N_{aug}}{u_{max} \cdot p_n} \qquad (3)$$

where N_{aug} and u_{max} are the tolerance for the augmented lagrangian solver (by default $N_{aug}=10^{-3}$) and the maximum displacement, respectively. For the present application, one may assume $u_{max}=w_{max}$.

Mesh was generated by fine-controlling element size (about 3mm) at plantar surfaces. Looking at Figure 6, one should note that the ground domain was meshed with hexahedral elements, while free tetrahedral elements were adopted for the foot geometry. Final mesh was made of 25812 nodes and 87149 elements. In order to reduce the computational effort, linear shape functions were adopted. Thus, the number of degrees of freedom of the FE model was 81428.

Numerical simulations were accomplished in about 100 min on a DELL Precision T7400 workstation (WinXP 64bit, 16GB RAM, 2 Xeon E5420 quad-core processors).

Figures 10 and 11 show the displacement field and the plantar pressure map, respectively. One should note that the maximum displacement is reached in the rear-foot area. Moreover, no relevant pressure is detected into the mid-foot area, whereas the maximum contact pressure of about 0.21 MPa happens, as expected, in the rear-foot area. So the calculated plantar pressure map may become a fundamental issue to be used when investigating perceived comfort at plantar-insole interface.

Future improvements of the present research will focus on the experimental validation of numerical results, by using high resolution insole sensors.

6. Final Remarks

The present paper focuses on the simulation of the balanced standing condition of a human foot model.

Once the 3D geometry of the human foot was generated from CT images, the non-linear FE model was built up. In particular, hyper-elastic material law and contact pairs were assigned in order to well capture the bio-mechanical behavior of the human foot when touching a rigid flat surface.

This research has highlighted some critical issues related to the analysis of a highly non-linear FE model in which complex geometry, hyper-elastic material and contacts are involved. The suggested parameters related to the best choice of the penalty factor as well as the settings of the solver come from some general rules along with a trial-and-error approach. This is true for several FEM-based software. All these fine-tuning operations are very time-consuming and there no guarantee of successful. So, some improvements and suggested best practices to resolve these kinds of problems are expected in the next future.

7. References

1. Jordan C., Barlett R., Pressure Distribution and Perceived Comfort in Casual Footwear, *Gait & Posture*, **Vol. 3**, Issue 4, pp. 215-220 (1995).
2. Whittle MW., Orofino TA., Miller K., Relationship between Mechanical Properties of Carpet and comfort in Walking, *Proc. of the Nacob II, The second North American Congress on Biomechanics*, Chicago (USA), August 24-28 (1992).
3. Channa P., Witana A., Ravindra S. Goonetilleke G., Shuping X., Effect of the Surface Characteristics on the Plantar Shape of Feet and Subjects Perceived Sensations, *Applied Ergonomics*, **Vol. 40**, Issue 2, pp. 267-279 (2009).

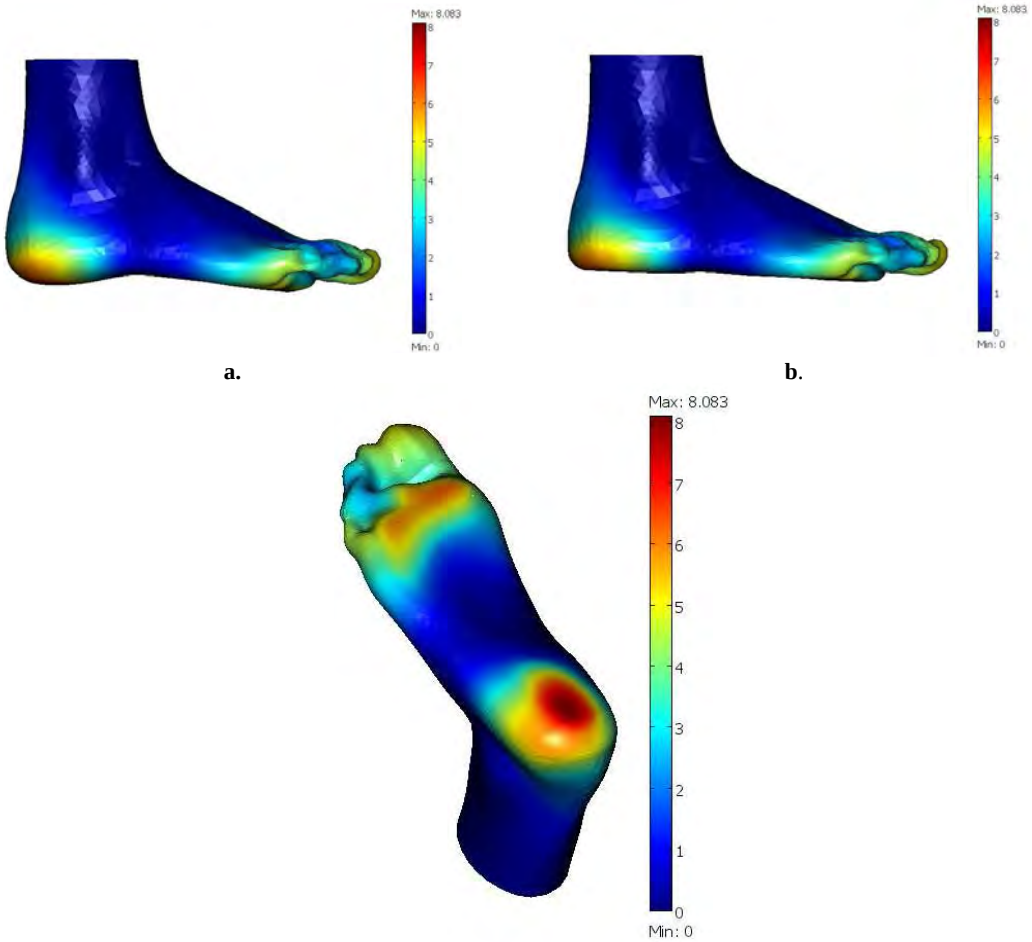

Figure 10. Domain contour plot for total displacement [mm].
a) undeformed geometry; b) deformed geometry, showed magnified 1x.

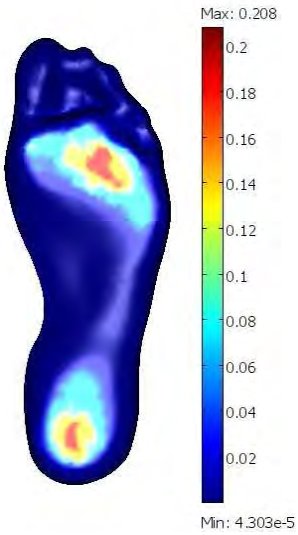

Figure 11. Boundary contour plot for pressure map [MPa]

4. Lee Yung-Hui, Hong Wei-Hsien, Effects of Shoe Inserts and Heel Height on Foot Pressure, Impact Force, and Perceived Comfort during Walking, *Applied Ergonomics*, **Vol. 36**, pp. 355–362 (2005).
5. Jason TM Cheung, Ming-Zhang, Aaron Kam-Lun Leung, Yu-Bo Fan, Three-dimensional Finite Element Analysis of the Foot during Standing: a Material Sensitivity Study, *Journal of Biomechanics*, **Vol. 38**, pp. 1045–1054 (2005).
6. Jason TM Cheung, Ming-Zhang, Parametric Design of Pressure-Relieving Foot Orthosis using Statistics-based Finite Element Method, *Medical Engineering & Physics*, **Vol. 30**, pp. 269–277 (2008).
7. Lemmon D., Shiang TY., Hashmi, A., Ulbrecht, JS., Cavanagh, PR., The Effect of Shoe Insoles in Therapeutic Footwear: A Finite Element Approach, *Journal of Biomechanics*, **Vol. 30**, pp. 615-620 (1997).
8. Wright DG, Rennels DC, A Study of the Elastic Properties of Plantar Fascia, *Journal of Bone Joint Surg Am.* **Vol. 46**, pp. 482-492 (1964)
9. Antunes PJ., Dias GR., Coelho AT., Reselo F., Pereira T., Non-Linear Finite Element Modelling of Anatomically Detailed 3D Foot Model, *technical report* (2008).
10. Jason TM Cheung, Ming-Zhang, A 3D Finite Element Model of the Human Foot and Ankle for Insole Design, *Archives of Physical Medicine and Rehabilitation*, **Vol. 86**, pp. 353-358, (2005).
11. Said R., Cotton R., Young P., Datta A., Elwassif M., Bikson M., Image Based-Mesh Generation for Realistic Simulation of the Tran-Cranical Current Stimulation, *Proc. of COMSOL Conference 2008*, Boston (2008).
12. Franciosa P., Gerbino S., Handling Tessellated Free Shape Objects with a Morphing Mesh Procedure in Comsol Multiphysics®, *Proc. of COMSOL Conference 2009*, Milano (Italy), October 14-16 (2009).
13. Jason TM, Cheung, Ming-Zhang, Finite Element Modeling of the Human Foot and Footwear, *Proc. of ABAQUS Conference 2006*, Cambridge-USA (2006).
14. Franciosa P., Martorelli M., Ausiello P., 3D Visualization and Fatigue Simulation in Restored Human Teeth by Using Micro-CT Data, *Proc. of the Int. ADM-INGEGRAF*, Lugo (Spain), June 10-12, (2009).
15. Wriggers P., *Computational Contact Mechanics*, Wiley, New York (2002).
16. Comsol Multiphysisc® 3.5a User Guide (Structural Mechanics Module – User's Guide).

8. Acknowledgements

Authors wish to express a warm thanks to dr V. Rufrano, from Univ. of Naples Federico II (IT), who accepted to undergo CT scan.
Many thanks also to dr. D. Speranza, from Univ. of Cassino (IT), for allowing us to use the Simplewere® package, and dr. F. Pepe and dr. G. Severino for their technical support.